Supporting information

Multilayer Two-Dimensional Water Structure Confined in MoS_2

Kijeong Kwac,[†] In Kim,[†] Tod A. Pascal,[⊥] William A. Goddard,[Δ] Hyung Gyu Park,[†,‡] and Yousung Jung[†,]*

[†] Graduate School of Energy, Environment, Water, and Sustainability (EEWS), and KAIST Institute NanoCentury, Korea Advanced Institute of Science and Technology (KAIST), 291 Daehakro, Yuseong-gu, Daejeon 34141, Republic of Korea

[⊥] Lawrence Berkeley National Laboratory, The Molecular Foundry, Berkeley, CA 94720, USA

[Δ] Materials and Simulations Process Center, Division of Chemistry and Chemical Engineering, California Institute of Technology, Pasadena 91125, USA

[‡] Nanoscience for Energy Technology and Sustainability, Department of Mechanical and Process Engineering, Eidgenössische Technische Hochschule (ETH) Zürich, Tannenstrasse 3, Zürich 8092, Switzerland

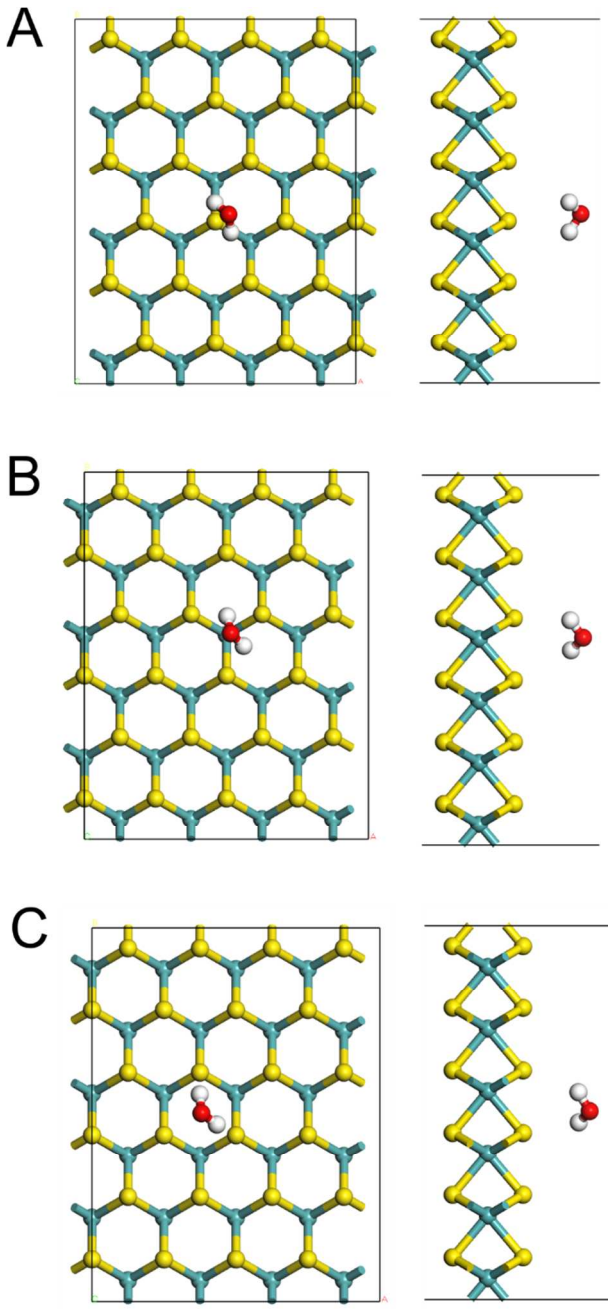

Figure S1. Three different configurations of a water molecule on a MoS_2 sheet.

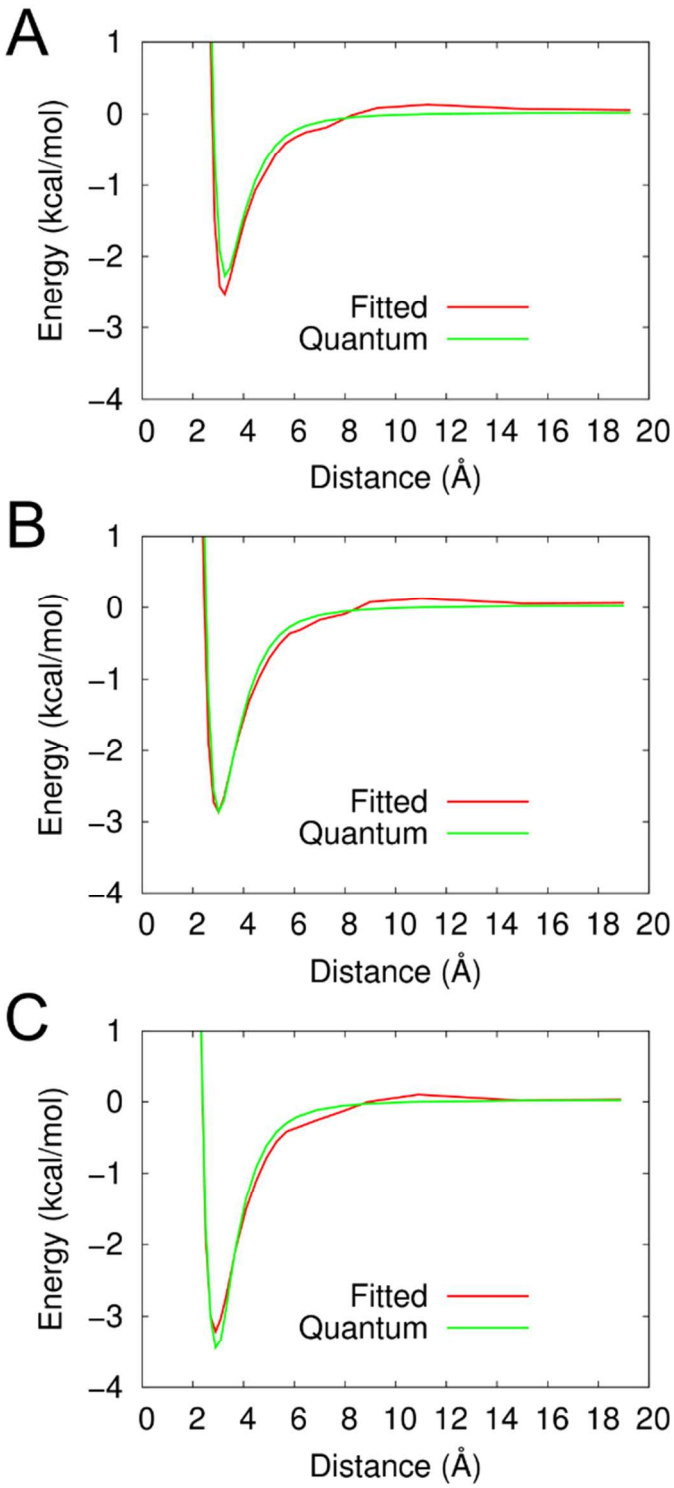

Figure S2. Comparison of the fitted Lennard-Jones potential with the potential energy curves obtained from electronic structure calculations as a function of the distance from the MoS_2 surface for the three different configurations of water molecules shown in Fig. S1.

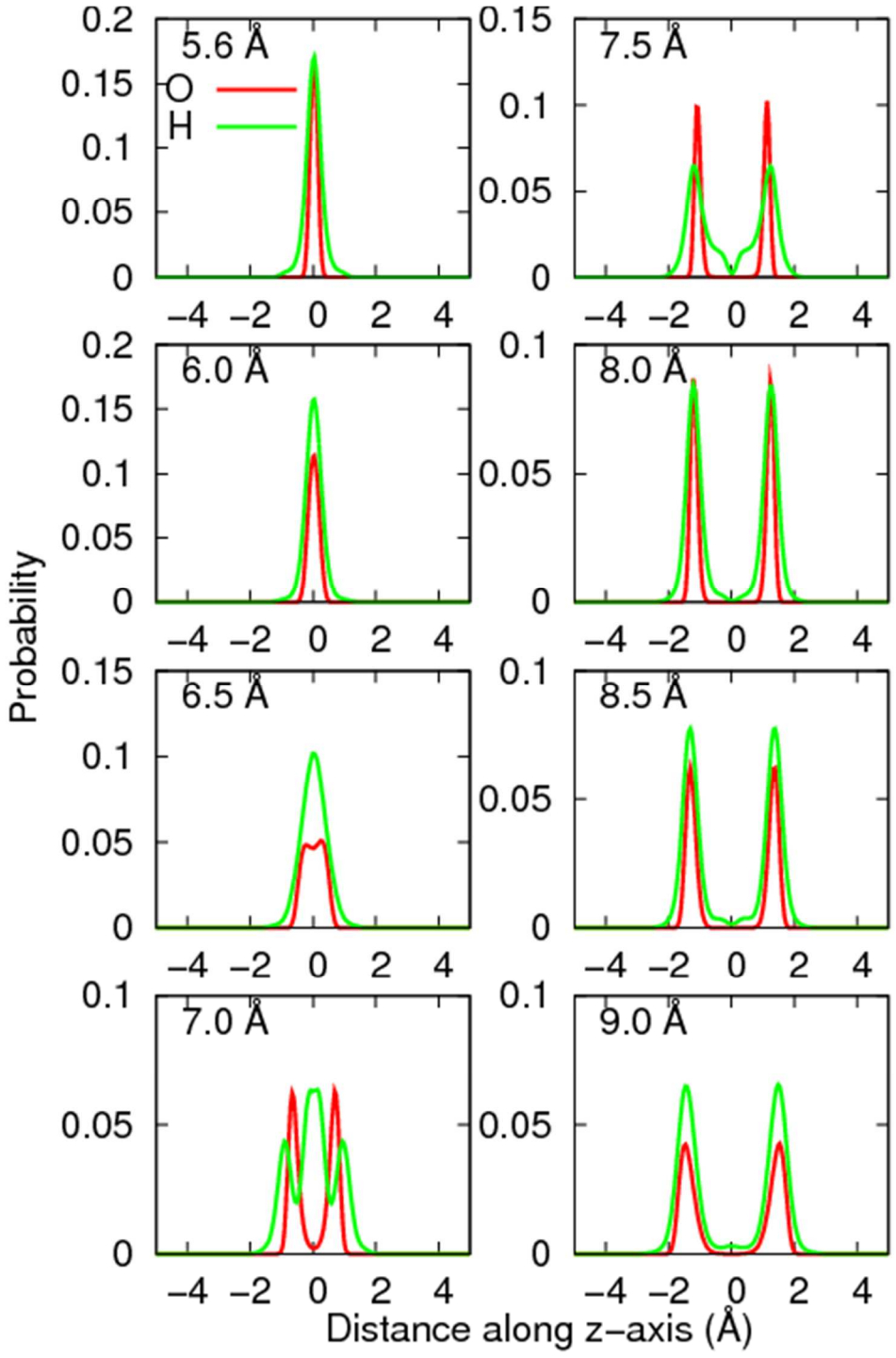

Figure S3. The number of water molecules between MoS_2 sheets as a function of z-position for the cases of gap spacing from 5.6 Å to 9.0 Å. z = 0 corresponds to the z-center of the gap spacing.

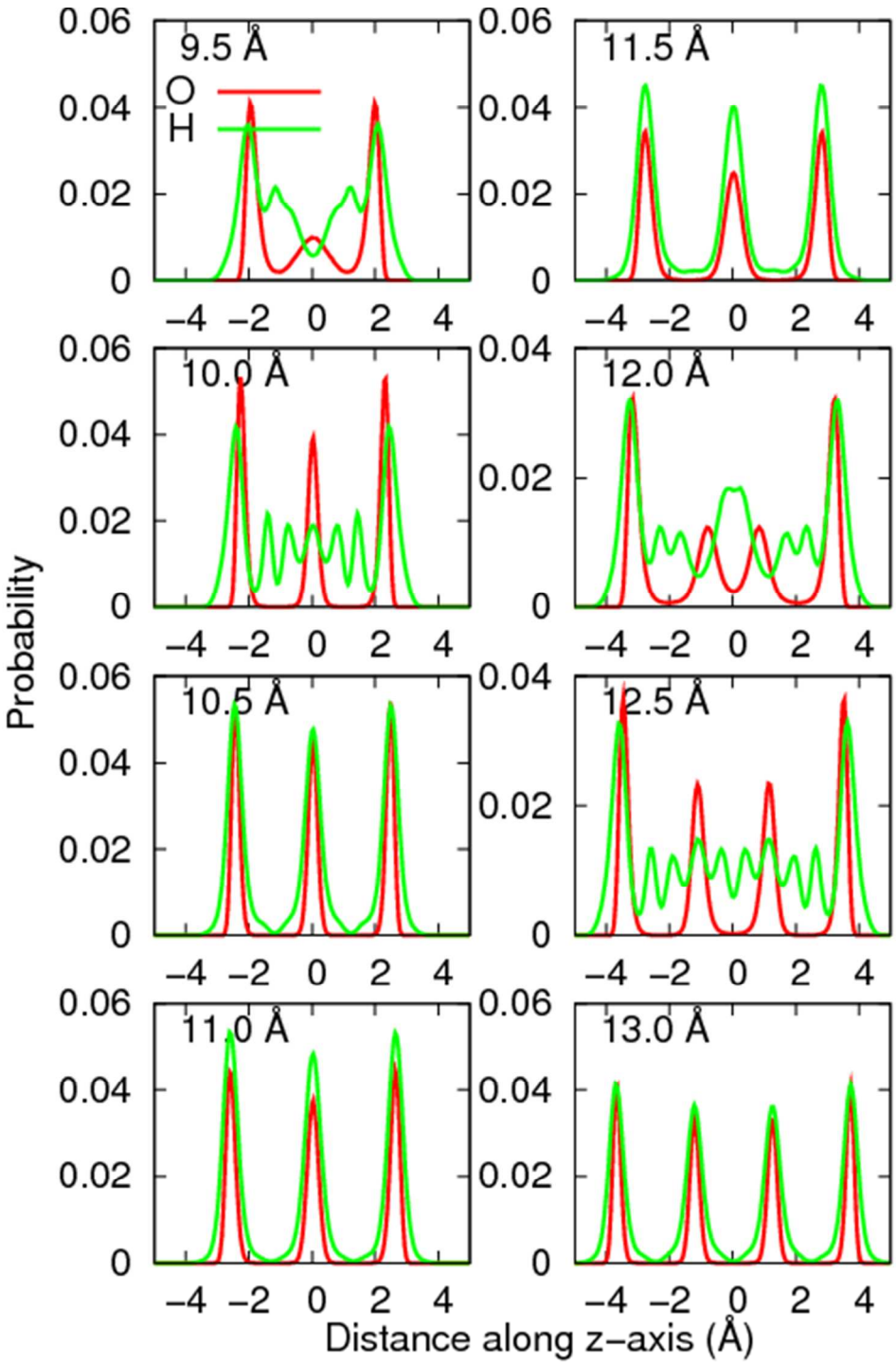
9.5 Å
O
H
11.5 Å
10.0 Å
12.0 Å
10.5 Å
12.5 Å
11.0 Å
13.0 Å
Probability
Distance along z–axis (Å)

Figure S4. The number of water molecules between MoS_2 sheets as a function of z-position for the cases of gap spacing from 9.5 Å to 13.0 Å. z = 0 corresponds to the z-center of the gap spacing.

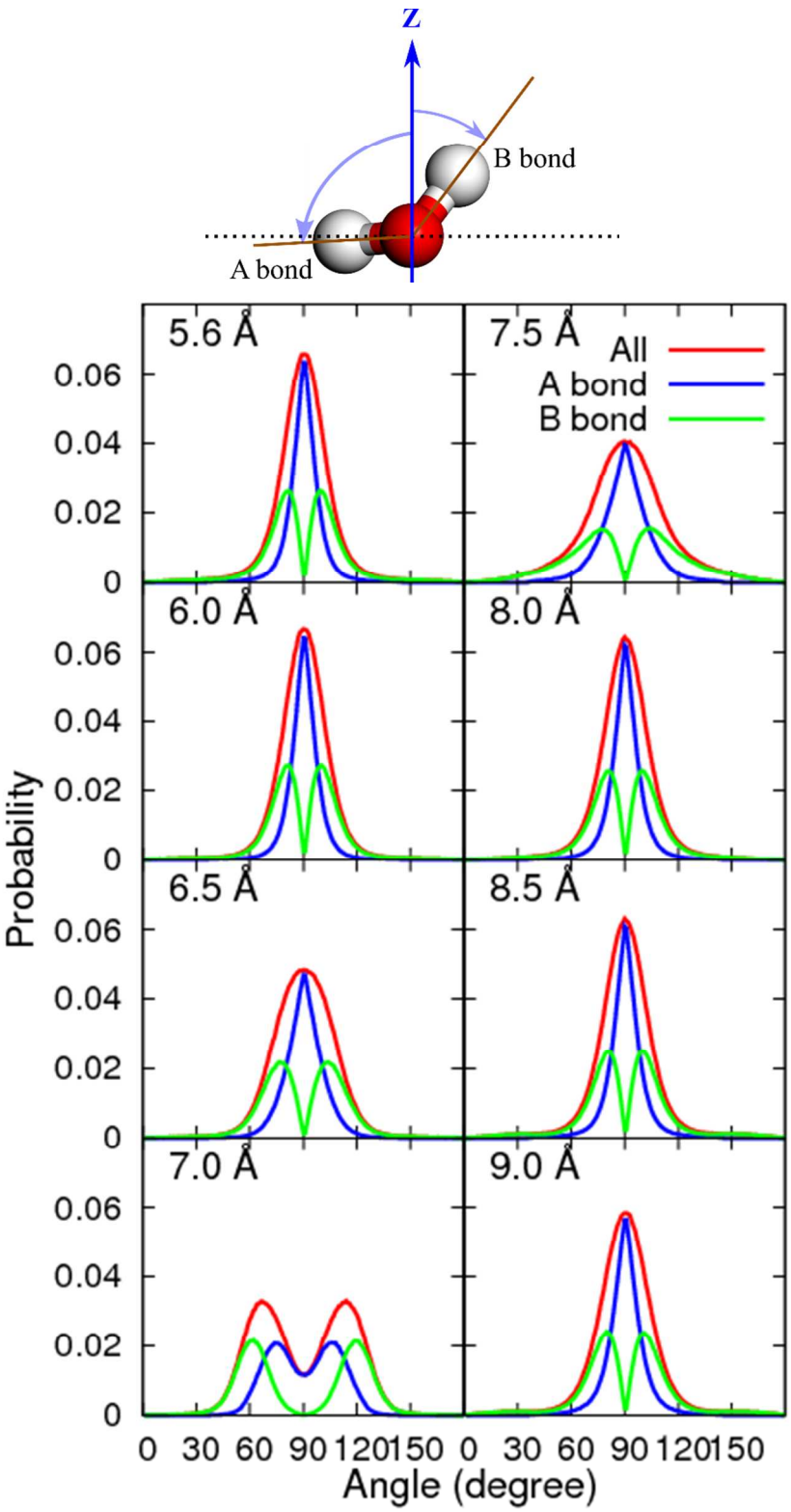

Figure S5. The probability distribution of the angle between the axis of the A and B bond and the z-axis for cases of gap spacing from 5.6 Å to 9.0 Å

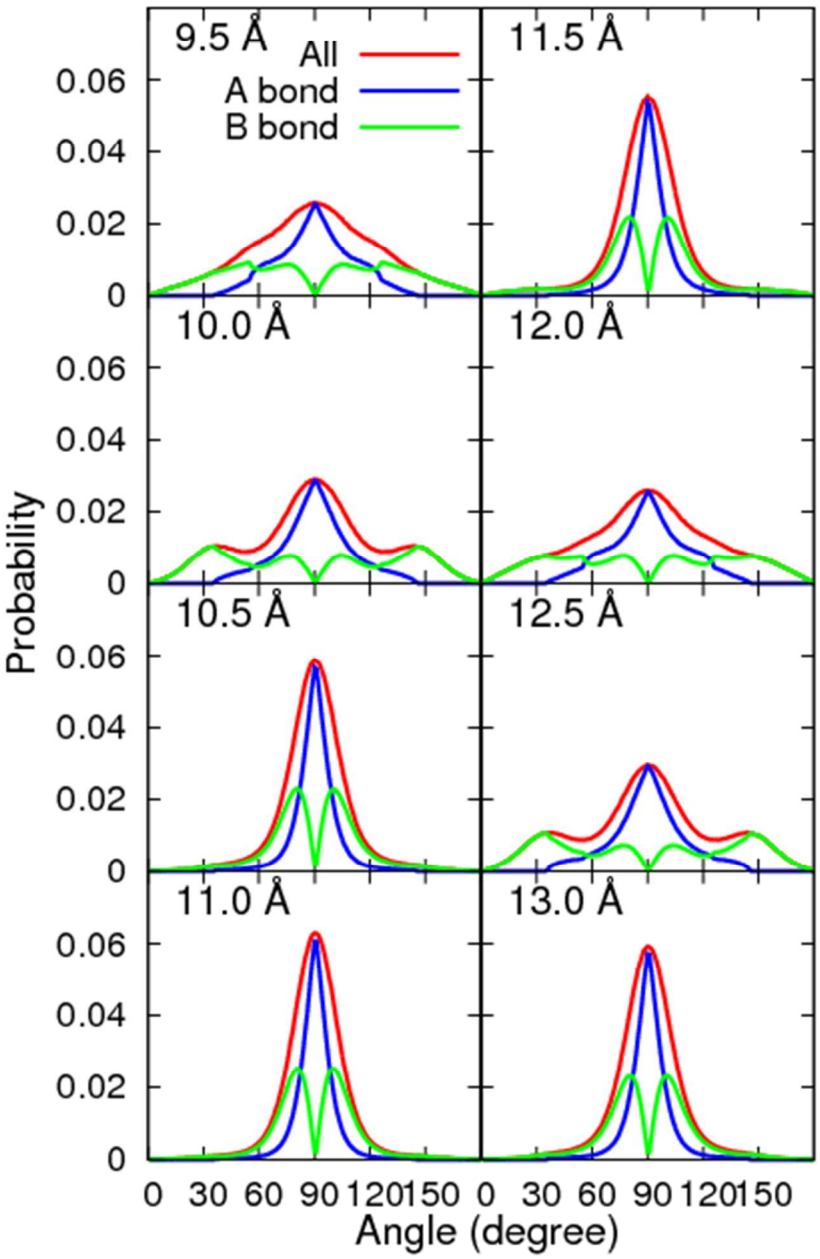

Figure S6. The probability distribution of the angle between the axis of the A and B bond and the z-axis for cases of gap spacing from 9.5 Å to 13.0 Å

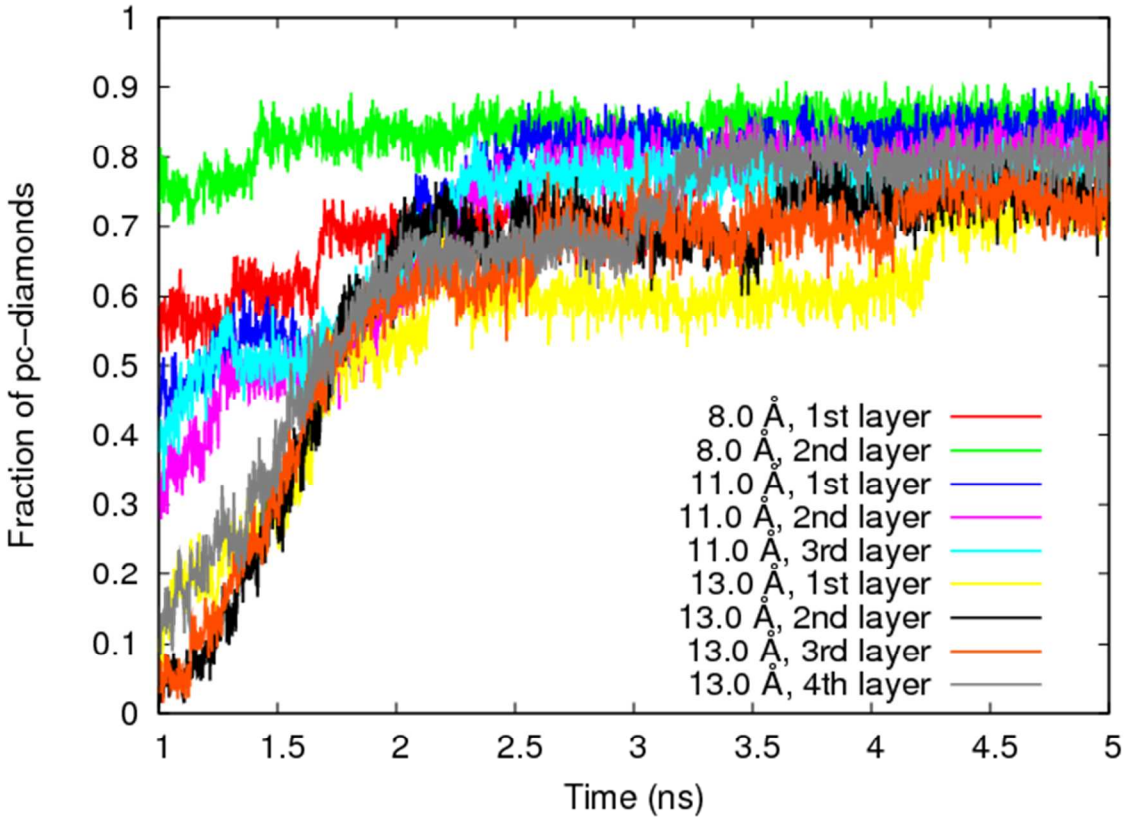

Figure S7. The fraction of water molecules participating in the configuration of the pc-diamonds structure during the 4 ns run after 1 ns equilibration.

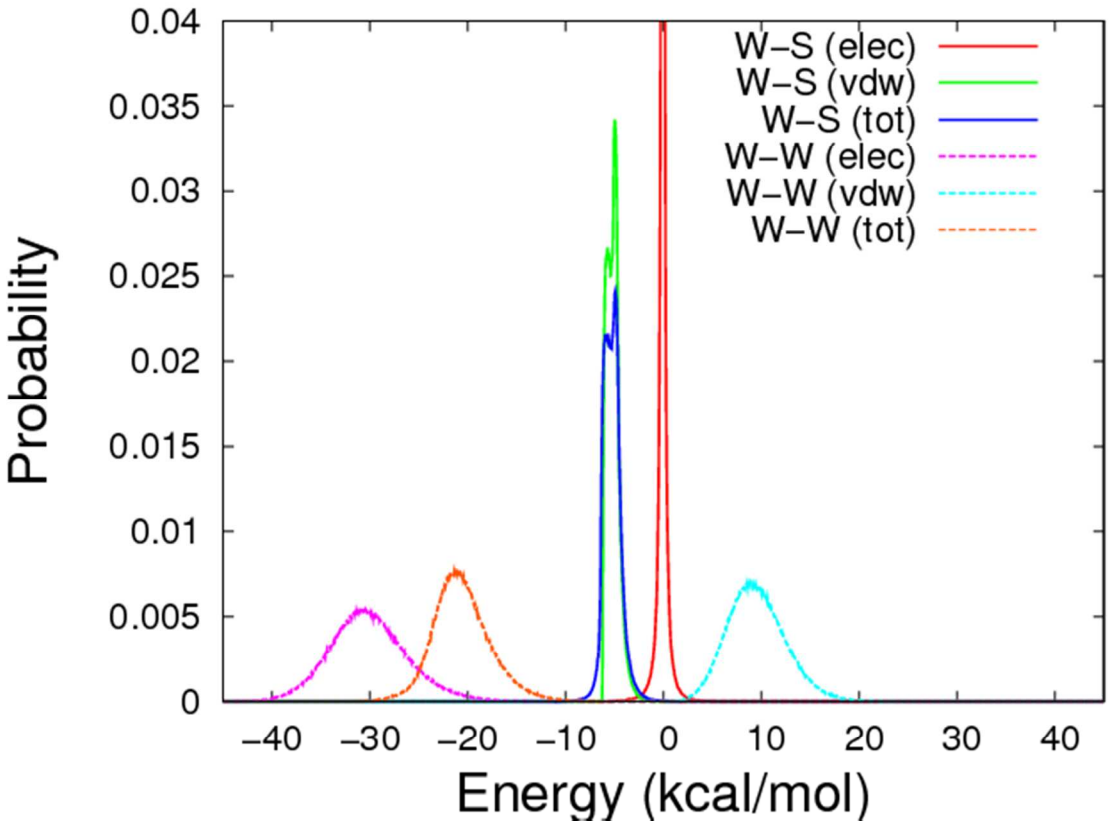

Figure S8. Contribution to the binding energy of electrostatic, van der Waals energies and the sum of the two energies for water – water (W – W) and water – MoS_2 (W – S) interaction.

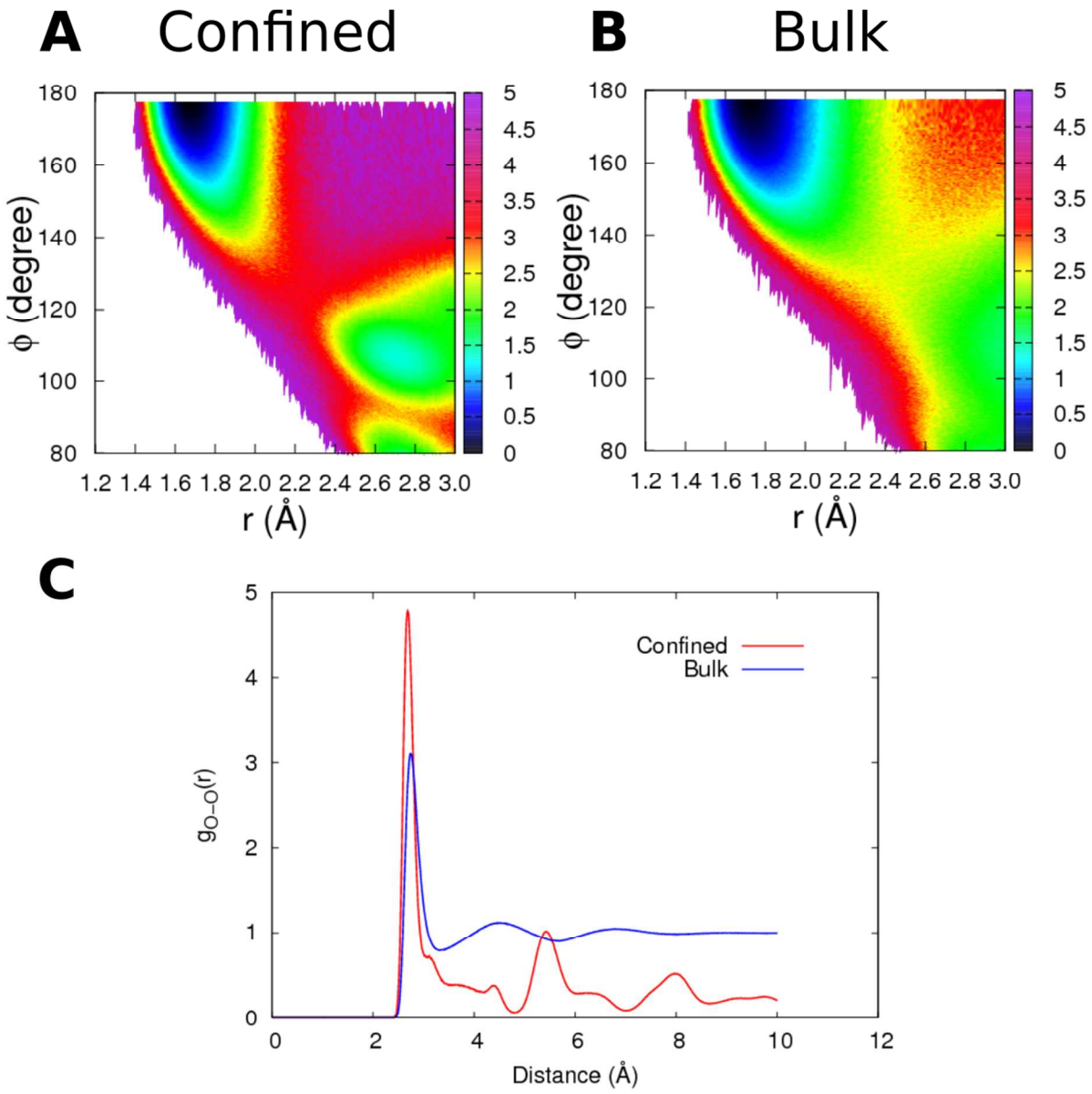

Figure 9. (A,B) The potential of mean force for the confined water between MoS_2 with 6.0 Å spacing and the bulk water as a function of the O…H distance *r* and the O – H…O angle φ. (C) Oxygen-oxygen radial distribution function of the confined water between MoS_2 with 6.0 Å spacing compared with that of bulk water.

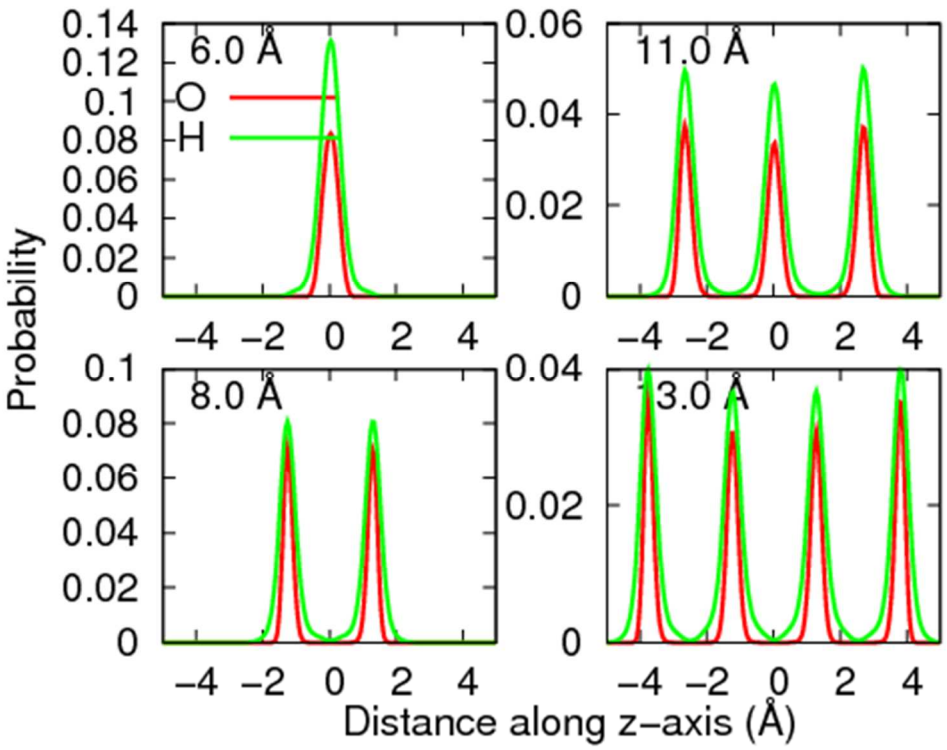

Figure S10. Number of water molecules between the confined region between the MoS2 sheets as a function of z-coordinates using the modified force field with 0.5ϵ for the Lennard-Jones potential between water and MoS_2.

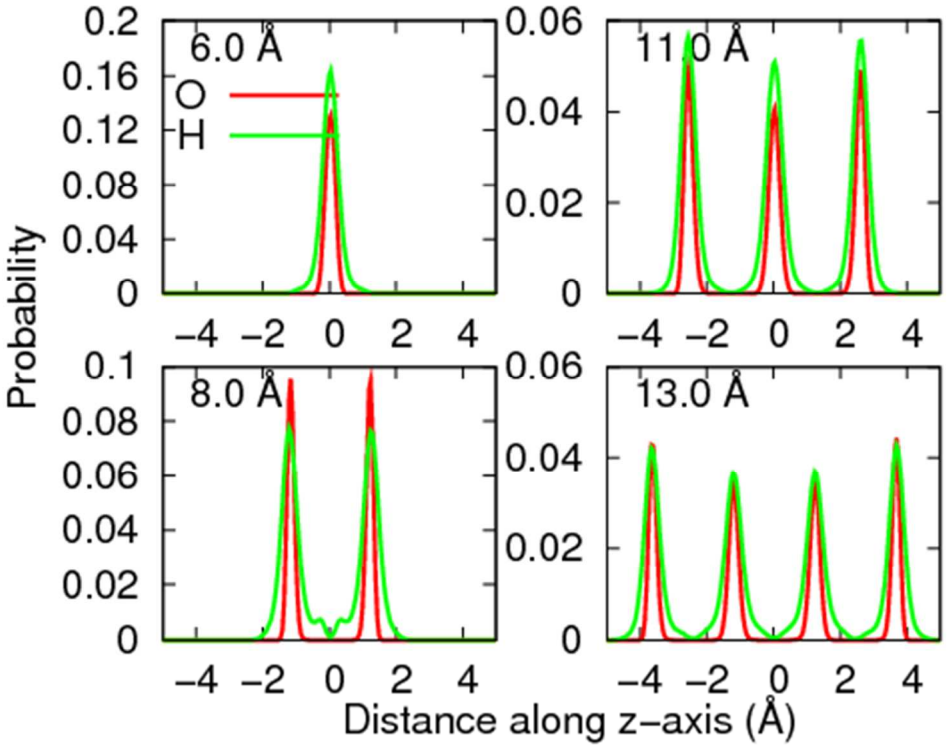

Figure S11. Number of water molecules between the confined region between the MoS2 sheets as a function of z-coordinates using the modified force field with 1.5ϵ for the Lennard-Jones potential between water and MoS_2.

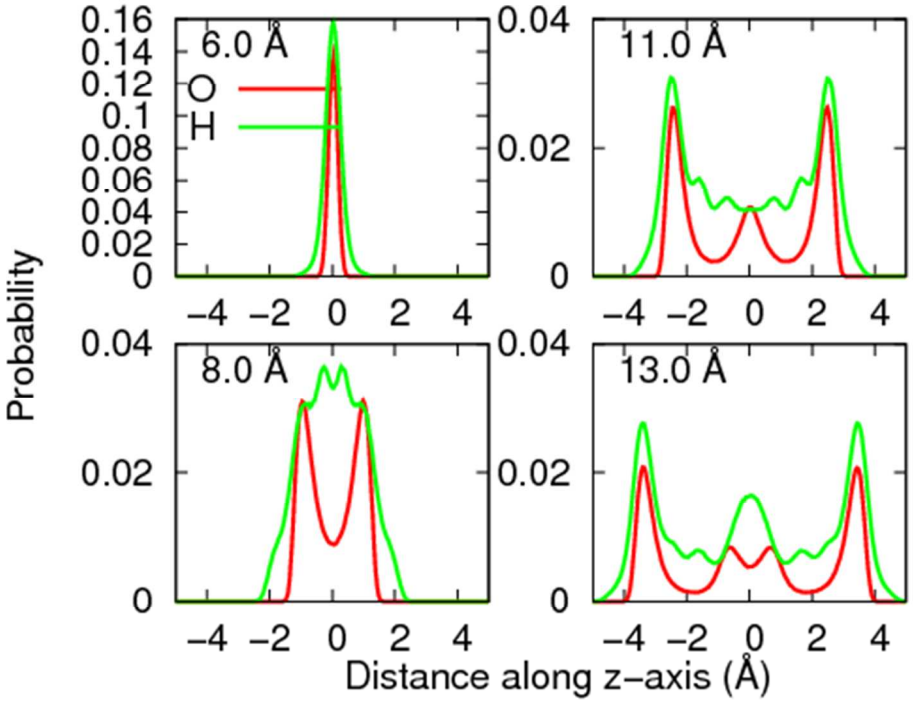

Figure S12. Number of water molecules between the confined region between the zero-charged MoS2 sheets as a function of z-coordinates. The distributions are calculated from 4 ns production run after 5 ns equilibration except the case of 6.0 Å in which we implemented 25 ns equilibration.

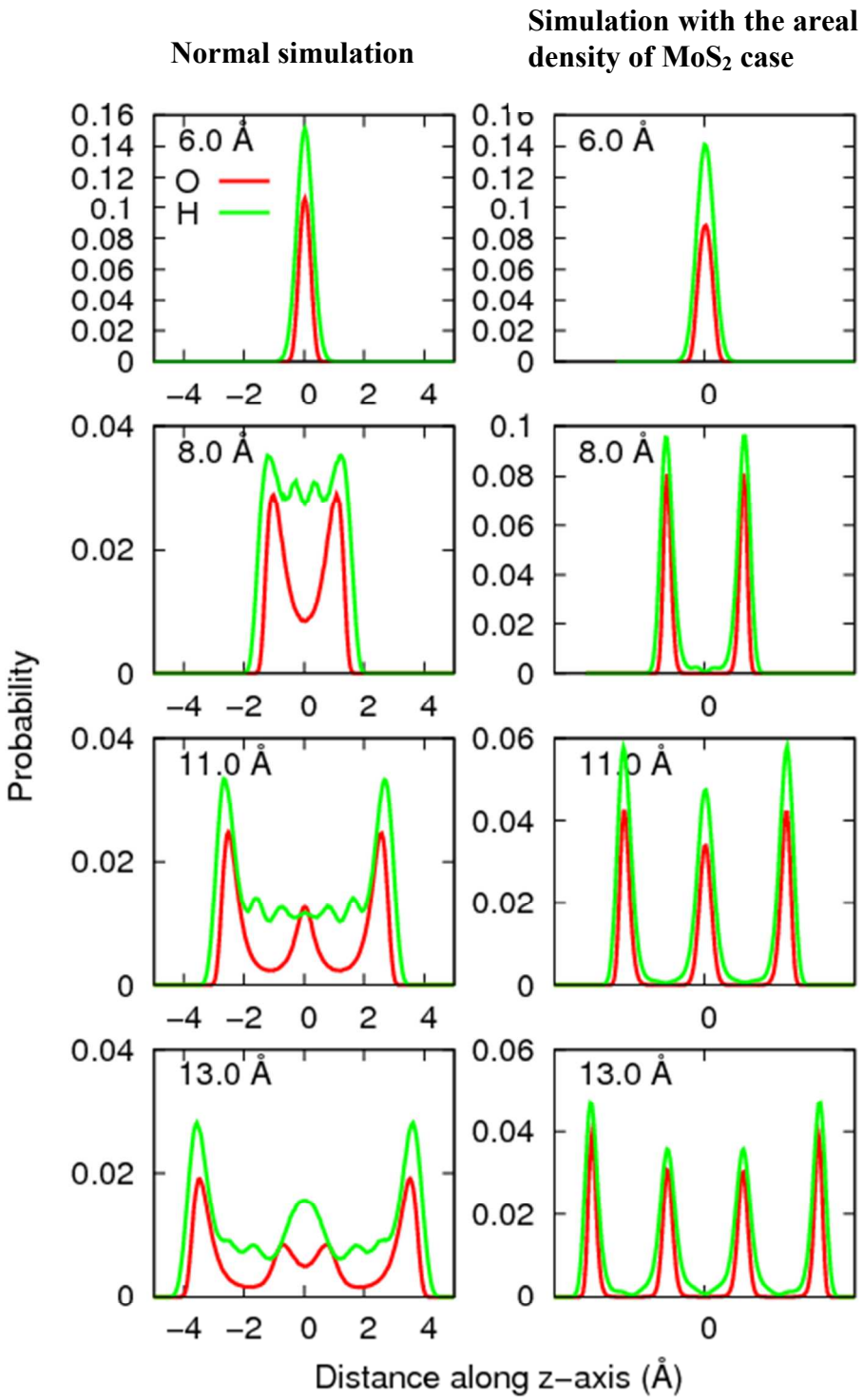

Figure S13. Density profile of water between graphene sheets for the normal simulation (left column) and the simulation (right column) in which the areal density of water molecules is set to be the same as the case of water between MoS_2 sheets with the same spacing.

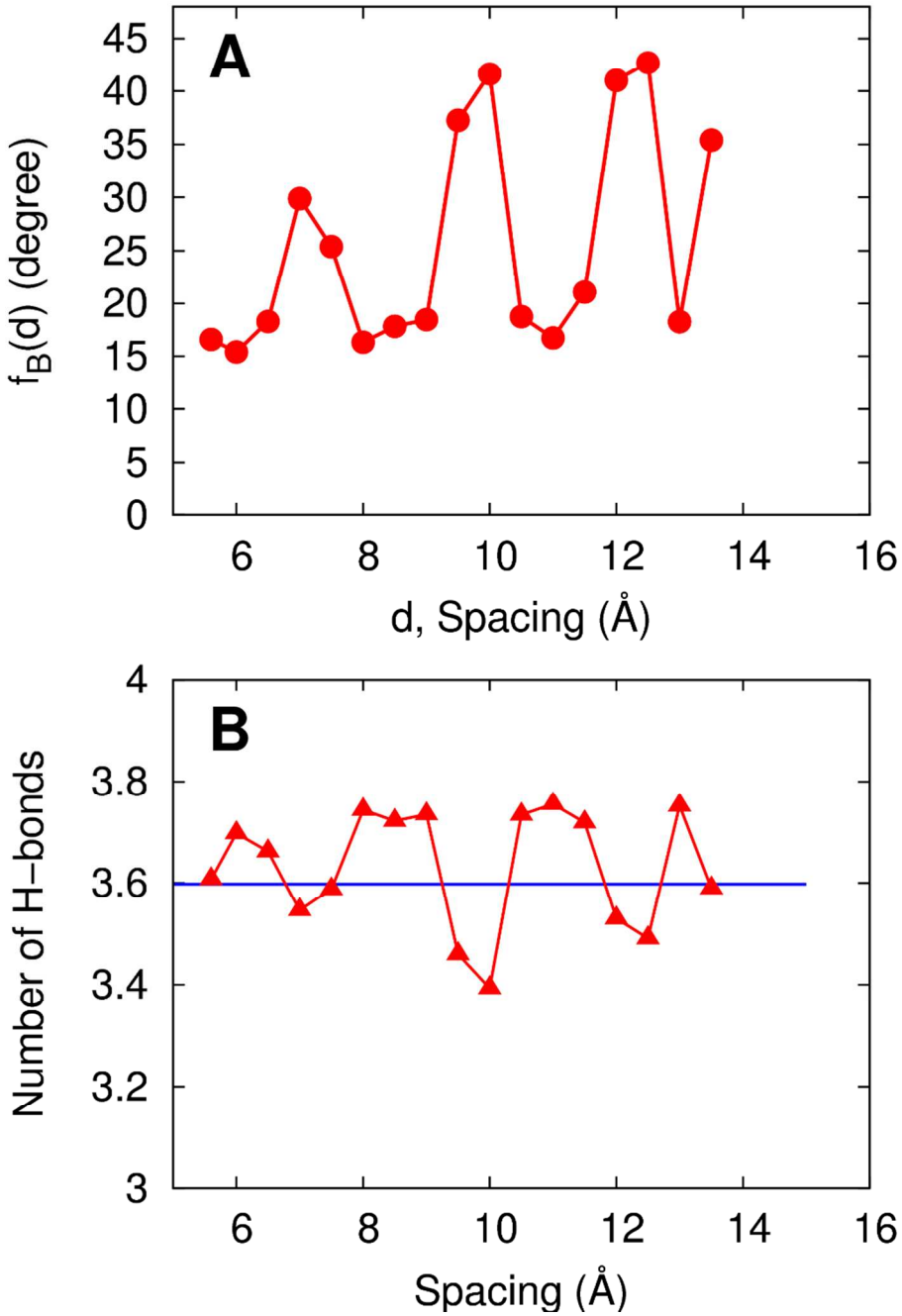

Figure S14. (A) The deviation of the angle between the B-bond axis and the z-axis from 90° as a function of the gap spacing of MoS_2 sheets. (B) The average number of hydrogen bonds per water molecule as a function of the gap spacing of MoS_2. The horizontal line at 3.6 is the average number of hydrogen bonds for bulk water.

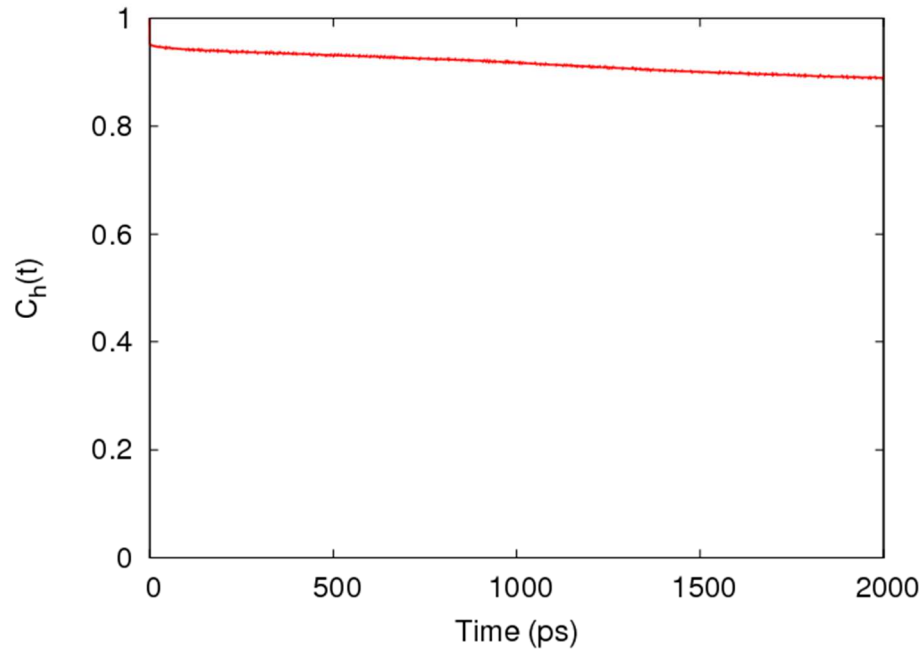

Figure S15. Plot of the time correlation function $C_{HB}(t)$ obtained from water between MoS_2 for 6.0 Å spacing.

Table S1. The force field parameters employed in the simulations. OI and HI represent the oxygen and hydrogen atom of hydroxide ions.

	q (e)	σ (Å)	ϵ (kcal/mol)
Mo	0.76 [1]	4.2 [2]	0.0135 [2]
S	-0.38 [1]	3.13 [2]	0.4612 [2]
C (graphene)	0.0	3.47299047 [3]	0.0951 [3]

Table S2. The Lennard-Jones parameters for the interaction of the selected pairs of atoms which do not use Lorentz-Berthelot combining rules. OW and HW represent the oxygen and hydrogen atom of water.

	σ (Å)	ϵ (kcal/mol)
C (graphene)−OW [4]	2.95	0.1132887
C (graphene)−HW [4]	2.80	0.0317878
Mo−OW	3.375674	0.237862
S−OW	3.499865	0.677863

Table S3. Volume density (g/cm^3) of water between MoS_2 with normal and modified force fields and water between graphene.

Spacing (Å)	MoS_2	MoS_2 (q = 0)	MoS_2 (1.5ϵ)	MoS_2 (0.5ϵ)	graphene
6	1.58	1.43	1.57	1.56	1.25
8	1.73	0.96	1.71	1.73	0.86
11	1.58	1.09	1.59	1.58	1.02
13	1.63	1.09	1.64	1.65	1.03

References for SI

1. Morita, Y., et al., Development of a New Molecular Dynamics Method for Tribochemical Reaction and Its Application to Formation Dynamics of Mos2 Tribofilm. *Applied Surface Science* **2008**, *254*, 7618-7621.
2. Liang, T.; Phillpot, S. R.; Sinnott, S. B., Parametrization of a Reactive Many-Body Potential for Mos2 Systems. *Phys. Rev. B* **2009**, *79*, 245110.
3. Mayo, S. L.; Olafson, B. D.; Goddard, W. A., Dreiding: A Generic Force Field for Molecular Simulations. *J. Phys. Chem.* **1990**, *94*, 8897-8909.
4. Pascal, T. A.; Goddard, W. A.; Jung, Y., Entropy and the Driving Force for the Filling of Carbon Nanotubes with Water. *PNAS* **2011**, *108*, 11794-11798.